Clays and Clay Minerals, Vol. 46, No. 2, 117–131, 1998.

STATE AND LOCATION OF WATER ADSORBED ON CLAY MINERALS: CONSEQUENCES OF THE HYDRATION AND SWELLING–SHRINKAGE PHENOMENA

R. PROST, T. KOUTIT, A. BENCHARA AND E. HUARD

Station de Science du Sol, INRA, Route de Saint-Cyr, 78000 Versailles, France

Abstract—The application of the Frenkel–Halsey–Hill (FHH) formalism to the water desorption isotherms obtained for the whole range of the activity of water with the pressure membrane device ($0.98 < a_w < 1$) and with the desiccator ($0 < a_w < 0.98$) gives information concerning the nature and the relative importance of the 2 mechanisms involved in the dehydration–hydration processes: adsorption and capillary condensation. The state and location of water are described in each domain. An equation that gives the thickness t of the film of water adsorbed on the walls of pores versus the activity of water is developed. This t-curve is used to get, from the desorption isotherm, the pore size distribution curve of the studied hydrated materials. Then concepts of surface and fabric of clay pastes are discussed as a function of hydration and a mechanism is proposed to explain swelling and shrinkage of finely divided materials. Three kinds of surfaces, related to the aggregate fabric, are defined as a function of their capacity to adsorb water. Each kind of surface is determined by a specific technique: the total surface area (S_t) by ethylene glycol adsorption, the external surface area of particles (S_s) by nitrogen adsorption and the external surface area of aggregates (S_e) by hydraulic conductivity measurements. As a consequence it is only with completely dispersed clays that swelling is a function of S_t. With unwell-dispersed clays, water adsorption, which induces swelling, successively occurs on S_t, S_s and S_e surfaces.

Key Words—Clay Paste Fabric, Hydration, State and Location of Water, Swelling and Shrinkage Mechanisms, t-Curve.

INTRODUCTION

The unique properties of clays mixed with water have permitted their use since the ancient times to make domestic objects and beautiful pottery. Although the physicochemical properties of clays as a function of water content have been known for a long time, it is a matter of fact that the mechanisms involved in their hydration, swelling and shrinkage are still not completely understood. The aim of this paper is to analyze data obtained by the senior author and his coworkers for a better understanding of the state and location of water retained by clay materials. The states of water are characterized by the mechanism (adsorption or capillary condensation) involved in the water retention phenomenon, and by the water–cation–clay structure interactions that determine the arrangement of water molecules with respect to solid surfaces, exchangeable cations and other water molecules. The location of water refers to sites or surfaces where water molecules are adsorbed and pores where water is condensed.

Determination of the affinity of clays for water will be discussed in the first part. Attention will be focused on the method developed to obtain a water desorption isotherm for the whole range of the activity of water ($0 < a_w < 1$). In the second part, we will show how the application of the FHH formalism to the water desorption isotherm gives information concerning the nature and the relative importance of the 2 mechanisms involved in the dehydration–hydration process: adsorption and capillary condensation. In the third part, the state and location of water will be described in each domain where 1 retention mechanism is predominant. In the fourth part, the concepts of surface and fabric of clay will be discussed as a function of hydration and a mechanism will be proposed to explain the swelling and shrinkage phenomena. Also, an overview will be presented concerning the effect of the structure of adsorbed water on the hydration process and, as a consequence, on the swelling phenomenon of clay materials. As oxides are commonly found in soils, they will be also taken into account.

CARRYING OUT OF WATER SORPTION ISOTHERMS FOR $0 < a_w < 1$

The water sorption isotherms give, for a given temperature, the amount of water retained by clay materials as a function of the activity of water (a_w). It is not possible to obtain a water sorption isotherm for $0 < a_w < 1$ performing only 1 experiment. Two methods are needed according to the range of a_w considered. For reasons of economy of space only typical data will be reported here. The reader may refer for more details to another paper by Prost (1990).

Carrying out Water Sorption Isotherms for $0 < a_w < 0.98$

Water sorption is generally performed in a desiccator where a_w is controlled by mixtures of H_2SO_4 +

Copyright © 1998, The Clay Minerals Society

https://doi.org/10.1346/CCMN.1998.0460201 Published online by Cambridge University Press

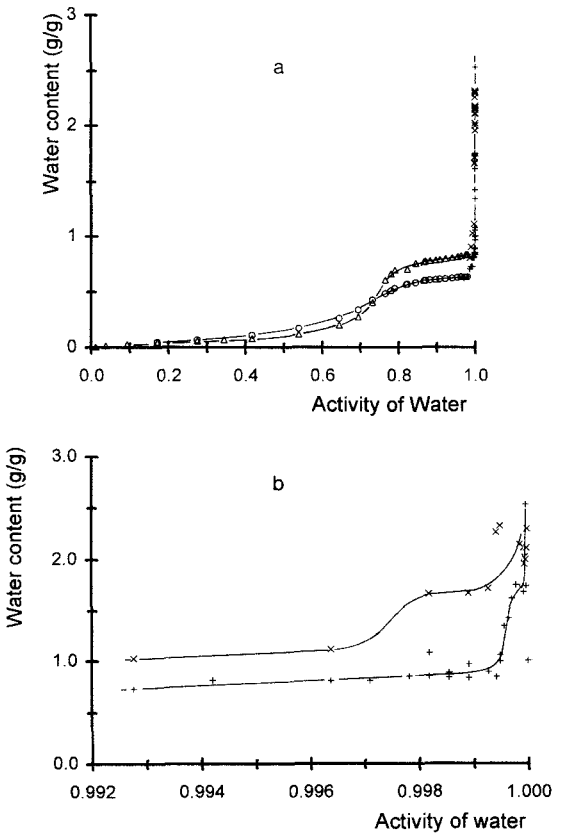

Figure 1. a) Water desorption isotherm of SiO_2 3–6 μm (data obtained with the pressure membrane device (×) and with the desiccator method (△)) and SiO_2 18–32 μm ((+) pressure membrane points, (○) desiccator points). b) Water desorption isotherm of SiO_2 3–6 μm (×) 18–32 μm (+) for $0.99 < a_w < 1$.

H_2O or saturated salt solutions. The desiccator is placed in a bath whose temperature is controlled. Difficulties arise due to condensation on the coldest point of the temperature controlling device when $a_w > 0.98$; therefore, the "desiccator method" allows accurate measurements only when $a_w < 0.98$.

Carrying out Water Sorption Isotherms for $0.98 < a_w < 1$

For sorption in the range $0.98 < a_w < 1$, filtration under pressure is used. Indeed, as has been shown by Sposito (1972) and Bourrié and Pédro (1979), the gas pressure P, applied in the so-called "pressure membrane device", is related to the free energy ΔG of the clay-water system by the following relationship:

$$\Delta G = -\bar{v}\, P = R\, T\, \mathrm{Ln}\, a_w \qquad [1]$$

where:

$\bar{v}$ is the partial molar volume of water,
R the gas constant,
T the temperature,

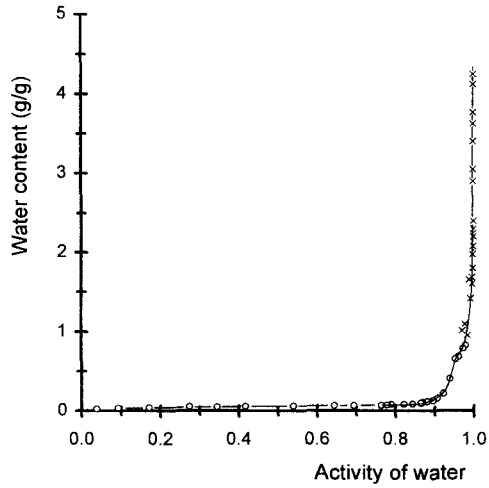

Figure 2. Water desorption isotherm of Al_2O_3 (data obtained with the pressure membrane device (×) and with the desiccator method (○)).

a_w the activity of water.

The pressure membrane device allows the control of a_w by the control of the applied pressure P. Pressures equal to 10 and 500 mbar correspond, according to Equation [1], to $a_w = 0.999993$ and $a_w = 0.999637$, respectively. Because it is easy to control such pressures, the pressure membrane device is well adapted to carry out water sorption isotherms for the highest values of a_w.

It is possible to carry out water adsorption isotherms with these 2 methods only if the suspension is free of salt (Koutit 1989). To avoid difficulties due to hysteresis, samples used in the desiccator method were prepared with the pressure membrane device under a pressure of 5 bars ($a_w = 0.996377$) (Prost 1990).

Figure 1a gives water desorption isotherms carried out with porous grains of SiO_2 used for chromatography. A good overlap of the data obtained with the pressure membrane and the desiccator device is noted. The isotherms, (Figures 1a and 1b), plotted with 2 different scales for a_w, clearly show the existence of 2 steps that are related to 2 different sets of constriction radii of pores. The step that occurs on the water desorption isotherm of both samples at $a_w = 0.75$ corresponds to the emptying of pores located inside the grains. The second step observed at $a_w = 0.9975$ and $a_w = 0.9995$ for 3–6 μm and 18–32 μm SiO_2 grains, respectively, corresponds to the emptying of larger pores related to the stacking or the fabric of the grains. The emptying of larger pores corresponding to larger grains occurs at a higher value of a_w than for smaller pores corresponding to smaller grains. Figure 2 gives the water desorption isotherm obtained with nonporous Al_2O_3 oxide grains whose specific surface area is

https://doi.org/10.1346/CCMN.1998.0460201 Published online by Cambridge University Press

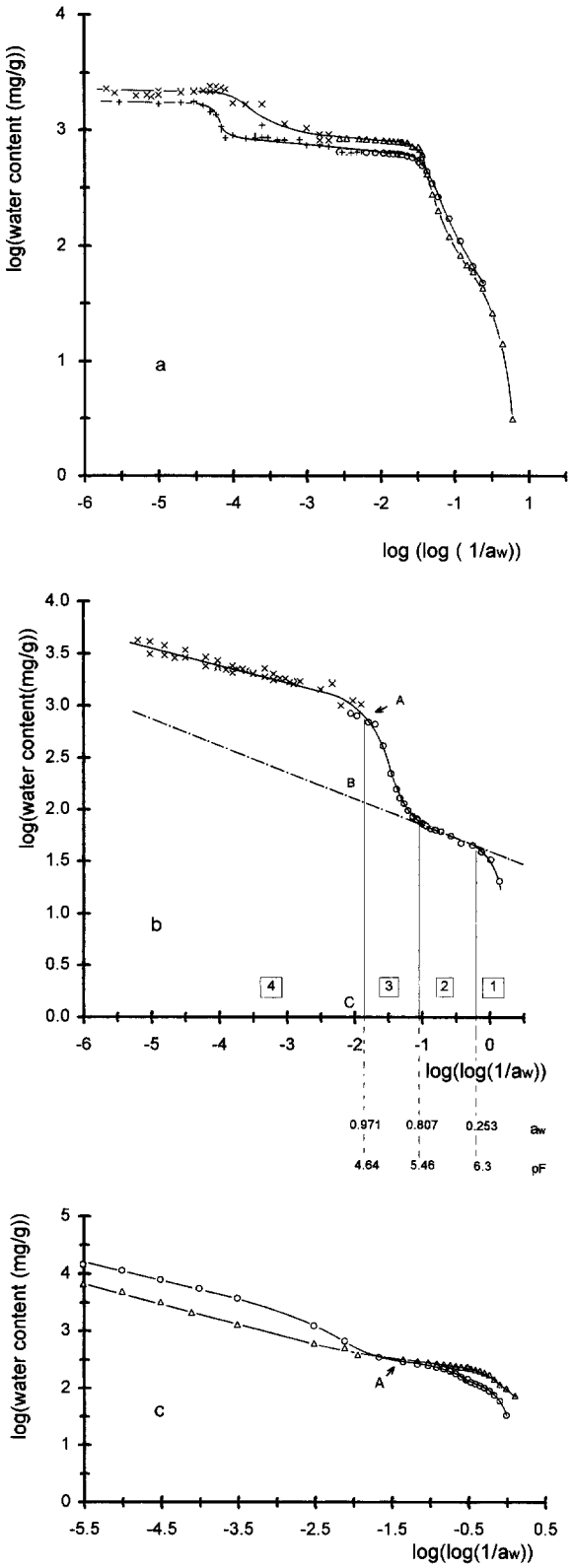

100 m^2 g^{-1}. Only 1 step is observed that corresponds to the fabric of particles in the pastes.

It is apparent from this that carrying out water desorption isotherms in the whole range of the activity of water can give the size of the constriction radii of pores (from the Kelvin equation, for example) and the porous volume of each set of pores involved in the retention mechanism of water.

STATES OF WATER RETAINED BY CLAY MATERIALS

Clay minerals and oxides are well known to retain large amounts of water relative to their mass; therefore, multilayer adsorption is assumed to be an operative mechanism in the water retention process. For this reason, we have applied a multilayer adsorption–desorption formalism to this process.

The FHH Equation

Frenkel (1946), Halsey (1948) and Hill (1952) showed, for intermediate values of a_w, that sorption isotherms can be described by the following equation:

$$\log\frac{p}{p_o} = \frac{k}{w^r} \qquad [2]$$

where: w is the water content, p/p_o the relative pressure of water and k and r constants that characterize the state of the solid surface and solute and the size and shape of the particles (Adkins et al. 1986).

The FHH curves are obtained plotting log w as a function of log (log(p_o/p)). This plot is similar to the plot of log w versus pF, which is commonly used in soil science. Here, we show that the usefulness of the FHH equation can be extended to the entire range of a_w from 0 to 1, obtained using the pressure membrane and desiccator methods.

FHH Plots of Finely Divided Materials

Figures 3a and 3b give the FHH plot for SiO_2 and Al_2O_3 pastes. The air-entry point, as determined by the Haines's plot (Haines 1923) occurs at a water content

←

Figure 3. a) FHH plots of SiO_2 3–6 μm (data obtained with the pressure membrane device (×) and with the desiccator method (△)) and SiO_2 18–32 μm ((+) pressure membrane points, (○) desiccator points). b) FHH plot of Al_2O_3 (data obtained with the pressure membrane device (×) and with the desiccator method (○)). A is the air-entry point. The numbers 1, 2, 3 and 4 correspond to domains where water retention is predominantly due to hydration of hydrophilic sites (1), multilayer adsorption (2), capillary condensation (3) and both multilayer adsorption and capillary condensation (4). The amount of water retained at a given a_w value by capillary condensation and adsorption are respectively represented by A − B and B − C. c) FHH plots of montmorillonite saturated by Na (○) and by Ca (△). A is the air-entry point.

https://doi.org/10.1346/CCMN.1998.0460201 Published online by Cambridge University Press

indicated on Figure 3b. The curve of Figure 3b is much simpler than the curves of Figure 3a obtained with SiO_2. Therefore, it will be used to describe the different states and location of water and also the mechanisms involved in the water retention phenomenon.

DOMAIN 1. It is observed for the lowest values of a_w and corresponds to water adsorbed on the hydrophilic sites of the material. In the case of clays these hydrophilic sites are exchangeable cations, cations of the edges and surface OH groups. Capillary condensation at contact points between particles may also occur at these low values of a_w (Prost 1975b).

DOMAIN 2. It corresponds to the multilayer adsorption process. It occurs on "free surfaces" (Pierce 1960), which are either walls of unsaturated pores or surfaces that belong to layers or particles that can expand freely.

DOMAIN 3. It begins when the FHH curve diverges from linearity as a_w increases. In this domain, capillary condensation of water in pores must be involved (Carott et al. 1982; Benchara 1991). The capillary condensation phenomenon occurs in pores that correspond to the fabric of hydrated particles.

DOMAIN 4. It corresponds to the part of the curve that is observed for the highest activities of water. This domain is related to the multilayer adsorption process on "free surfaces" of grains or particles and to a capillary condensation mechanism in saturated pores whose size increases or decreases as swelling or shrinkage occurs.

Figure 3a gives the FHH plot of SiO_2 3–6 μm and SiO_2 18–32 μm samples. Several domains are observed that correspond to different states of water in these materials. The steps of the FHH curves, observed for the highest water contents, occur at different values of a_w for the 2 samples because the size difference leads to unique fabric structures for each particle size.

Figure 3c shows the FHH plots of Na- and Ca-montmorillonites. The air-entry point occurs at low water contents for Na-montmorillonite (Tessier 1984). The S-shaped part of the curve, which occurs while the Na-montmorillonite is saturated, is attributed to the contraction of the interlamellar spaces from 4 to 2 nm (Norrish 1954).

In general, the FHH formalism allows us to analyze water retention in terms of 2 different mechanisms:

1) *adsorption,* which occurs on hydrophilic sites at the lowest value of a_w or on "free surfaces" for higher values of a_w;

2) *capillary condensation,* which occurs at contact points between particles at the low values of a_w or in pores at the high values of a_w.

As a result, the state of water can be defined by the energy of hydration, which is related to a_w by the mechanisms involved in the hydration process, and by the location of water in the paste. The energy of hydration is obtained from a_w and each domain defined by the FHH plot is characterized by a range of a_w. The mechanisms involved are adsorption and capillary condensation. The location and the amount of water adsorbed or condensed at each value of a_w can be specified with the FHH plot.

Jurinak (1963) applied the FHH formalism to the water adsorption isotherm obtained for kaolinite. He found a linear relationship for $0.2 < a_w < 0.97$, which is expected for the multilayer adsorption process in this range of a_w. Prost (1990), applying the FHH formalism to the water desorption isotherm of kaolinite, obtained in the whole range of the activity of water ($0 < a_w < 1$), concluded that the multilayer adsorption process is predominant in a larger range of a_w for the <50 μm fraction of kaolinite than for the <1 μm fraction.

In domain 3, where capillary condensation occurs in pores resulting from the fabric of finely divided particles (Al_2O_3 oxide, kaolinite, . . .), both water retention phenomena exist: capillary condensation and multilayer adsorption. Pierce (1953) has used the same mechanisms to describe the desaturation process of porous materials saturated by liquid nitrogen. Our hypothesis is that the multilayer adsorption process exists in domains 2, 3 and 4, following the same linear relationship, even when finely divided materials are saturated by water rather than nitrogen.

So the FHH plot allows the determination of the amount of water retained by adsorption and by capillary condensation. Figure 3b shows how these determinations can be made for each value of a_w. At the air-entry point 70% of the amount of water, represented by A − B, is located in large pores whose size can be determined by the method described in the following paragraph.

Structure of Gels and Pastes of Finely Divided Materials

Hydraulic conductivity measurements performed on saturated pastes corresponding to domain 4 (Prost 1990) give indications of the mean hydraulic radii of pores as a function of water content. The application of an equation developed by Prost (1990) allows the calculation of the specific surface area S_e of grains and aggregates. The good agreement observed (Table 1) for well-dispersed materials (Al_2O_3, chrysotile, kaolinite at pH = 9) between specific surface area determined from the nitrogen adsorption isotherms, using the Brunauer, Emmet and Teller formalism (BET method), and from the hydraulic conductivity measurements, suggests that water flows between individual particles. The lower specific surface area deter-

https://doi.org/10.1346/CCMN.1998.0460201 Published online by Cambridge University Press

Table 1. Specific surface area S_s (BET method), S_e (Hydraulic conductivity method) and amount of water w_o located in the porosity of aggregates or flocculates.

Samples	S_s ($m^2\ g^{-1}$)	S_e ($m^2\ g^{-1}$)	w_o ($g\ g^{-1}$)
Al_2O_3	100	100	0
Chrysotile	34	27	0
Kaolinite pH = 9	19	20	0
Kaolinite pH = 5.6	19	6	0.32

mined by hydraulic conductivity for kaolinite at pH = 5.6 (Table 1) arises from the flocculation of the suspension and to the fact that water flows between flocculates.

Application of the formalism developed by Pierce (1953) for nitrogen desorption isotherms and adapted to water desorption isotherms, allows the determination of the pore size distribution curves of wet materials. This formalism, which implies a knowledge of the "*t*-curve", was applied to domains 3 and 2 of the FHH plot where desaturation occurs.

Because finely divided materials are not rigid porous media, the pore size distribution curves from water desorption are slightly transformed relative to those obtained with mercury injection. Such pore size distribution curves (Figure 4) give values of constriction radii of wet systems which are, of course, slightly underestimated compared to the original paste. Nevertheless, they clearly show that water retained in SiO_2 3–6 μm grains by capillary condensation is located in large pores, whose constriction radii are around 350 nm, and in small pores, whose constriction radii are close to 4 nm. The larger constriction radii (450 nm) observed on the pore size distribution curve obtained by mercury injection compared to the one deduced from the water desorption isotherm (350 nm) is due to the relaxation of the structure of the solid phase when the film of water causing cohesion between particles is removed.

In summary, the FHH plot applied to water desorption isotherms obtained in the whole range of the activity of water gives qualitative and quantitative indications about the state and location of water (adsorbed on hydrophilic sites or on "free surfaces" and condensed in large pores) in pastes made of finely divided materials. The next section will be devoted to the structure of water near solid surfaces in order to understand the hydration process of these finely divided materials at the molecular level.

STRUCTURE OF WATER ADSORBED ON CLAY MATERIALS

The structure of adsorbed water on clay materials is defined as the way water molecules are arranged near clay surfaces. To do so, we will first consider the structure of bulk water or ice.

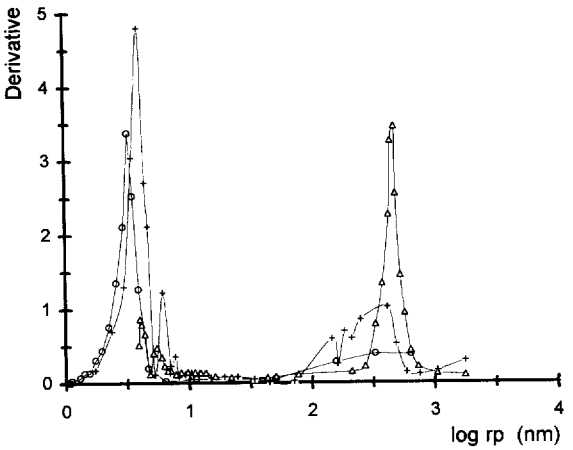

Figure 4. Pore size distribution curves of SiO_2 3–6 μm obtained from the water desorption isotherm (+), mercury injection (△) and from the nitrogen desorption isotherm (○).

Eisenberg and Kauzmann (1969) developed an original concept for the structure of bulk liquid water based on the time scale that is specific to each technique used as a probe. On a time scale that is long relative to the period of vibration of a hydrogen bond in liquid water (about 10^{-13} s), but short relative to the time required for a water molecule to diffuse a distance equal to its own diameter (about 10^{-11} s), a typical molecule in liquid water "sees" a spatial arrangement of its neighbors that is called the vibrationally averaged structure (V-structure). This structure will include only the effects of vibrational motions of the water molecules and, according to Figure 5, can be probed by infrared (IR), neutron scattering and nuclear magnetic resonance (NMR) spectroscopy. At the other extreme, on a time scale that is long compared with that during which a molecule diffuses a nominal distance in liquid water, a typical molecule "sees" a surrounding spatial arrangement that is called the diffusionally averaged structure (D-structure). This structure includes the effects of vibrational, rotational and translational motions of the water molecules and will be more ordered than the V-structure because it comprises only the most probable molecular configurations. The D-structure can be probed by neutron and X-ray diffraction (XRD) experiments, and it provides a basis in molecular structure for thermodynamic properties, as suggested in Figure 5.

Between the time domains of the V- and D-structures, there is a transition region that can be investigated by neutron scattering, NMR and dielectric relaxation spectroscopy. These techniques are expected to give information about the rotational and translational motions of water molecules that lead from the V-structure to the D-structure. Thus, it is clear that the concept of "structure" in liquid water is a *dynamic* one,

https://doi.org/10.1346/CCMN.1998.0460201 Published online by Cambridge University Press

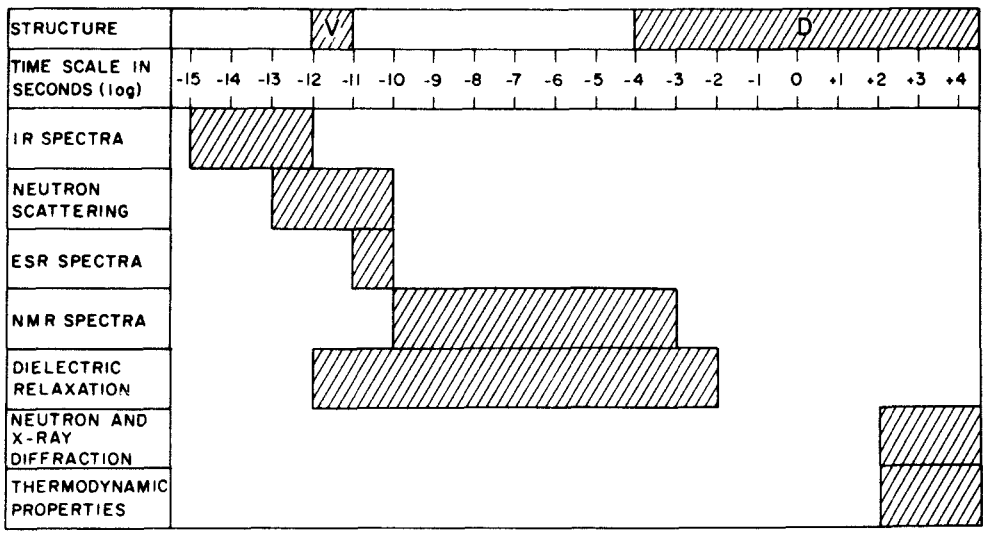

Figure 5. Time scales for adsorbed water structures and the experimental methods used to measure the properties of adsorbed water (Sposito and Prost 1982).

and the same should be true for the water adsorbed by clays.

In the case of adsorbed water, an additional complexity is provided by the exchangeable cations, whose vibrational and translational motions take place in the transition region between the V- and D-structures. Solid state NMR of exchangeable cations such as Li, Na, Cs, Cd and K may contribute to a better understanding of the water–cation–clay structure interactions.

The review by Sposito and Prost (1982) gives the basic results concerning the structure of water adsorbed on clay surfaces. For reasons of economy of space, data and discussions developed in that review concerning IR spectroscopy, neutron scattering, NMR spectroscopy, dielectric relaxation, neutron and XRD and thermodynamic properties will not be reported here. Data obtained by solid state NMR and far-IR spectroscopy, which allow one to probe the surface through the exchangeable cations, will be presented. Taking into account all these data, a synthetic structure of adsorbed water will be given.

Solid-State NMR and Far-IR Spectroscopy of Compensating Cations

A high-resolution solid-state NMR study of exchangeable cations in the interlayer space of Llano vermiculite saturated by Na, Cd and Cs (Laperche et al. 1990) shows that each phase (dehydrated, 1-layer hydrate and 2-layer hydrate) identified by X-ray is characterized by a unique chemical shift δ_{CG} (CG: center of gravity of the line) and by a typical bandwidth $\nu_{1/2}$. On Figure 6 are gathered spectra of the different phases of Na-vermiculite. All spectra may be accounted by 1 or 2 lines among 3 possible contributions: one corresponding to the 2-layer hydrate (δ_{CG} = 4,5 ± 0,5 ppm), one to the 1-layer hydrate (δ_{CG} = −7 ± 1 ppm) and one to the dehydrated phase (δ_{CG} = −18 ± 1 ppm). The analysis of the data leads to the conclusion that Na cations are located in 2 different sites in the 1-layer hydrate and in consequence are solvated by 2 populations of water molecules. Such a conclusion was reached by the simultaneous analysis of ^{1}H and ^{23}Na NMR spectra of the 1-layer hydrate (Laperche et al. 1990).

A variable-temperature MAS NMR study of ^{133}Cs-hectorite led Weiss et al. (1990a, 1990b) to assign the 2 peaks observed for clay–water slurries to Cs atoms in the Stern layer and in the Gouy diffuse layer. The peak ascribed to Cs in the Stern layer is not affected by Cs concentration, whereas the peak ascribed to Cs in the Gouy diffuse layer changes with increasing Cs concentration in the bulk solution with which the clay equilibrated. The 2 peaks observed for fully dehydrated samples were assigned to 2 different interlayer sites.

Lambert et al. (1992) report data obtained with a K-montmorillonite submitted to wetting and drying (W-D) cycles. Figure 7 gives ^{39}K solid-state NMR spectra of potassium in montmorillonite pastes prepared with samples submitted to 0, 11 and 100 W-D cycles and after a replacement of exchangeable K by Sr in the 100 W-D sample. Spectra were deconvoluted into a narrow and a wide peak. When the number of W-D cycles increases, the intensity of the wide peak increases. The narrow peak is assigned to K hydrated by more than 3 water molecules, and the wide peak to K which is hydrated by less than 3 water molecules. So the proportion of K hydrated by less than 3 water molecules increases as the number of W-D cycles increases. The narrow peak disappears when exchangeable K

https://doi.org/10.1346/CCMN.1998.0460201 Published online by Cambridge University Press

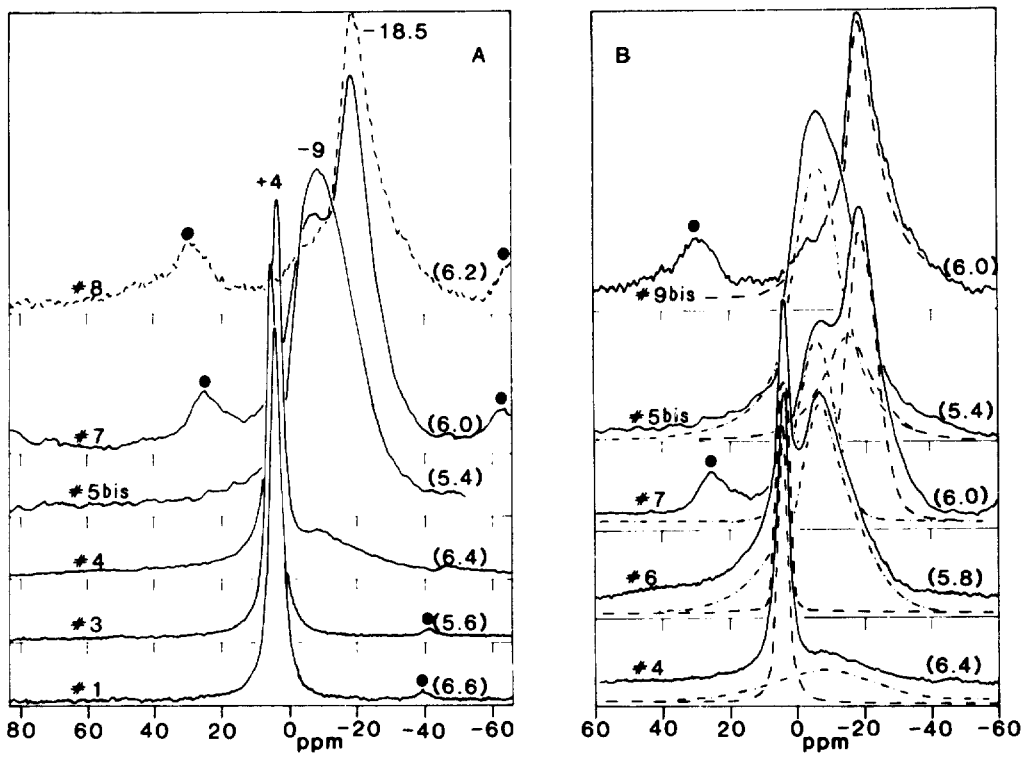

Figure 6. A) ^{23}Na MAS NMR spectra at different hydration levels. The spinning rate (kHz) is indicated between parentheses. Circles show the spinning sidebands. B) ^{23}Na MAS NMR spectra for biphasic samples at large scale (solid line). The dashed or interrupted lines show the deconvolution into 2 components. The areas under these lines are their relative contributions (Laperche et al. 1990).

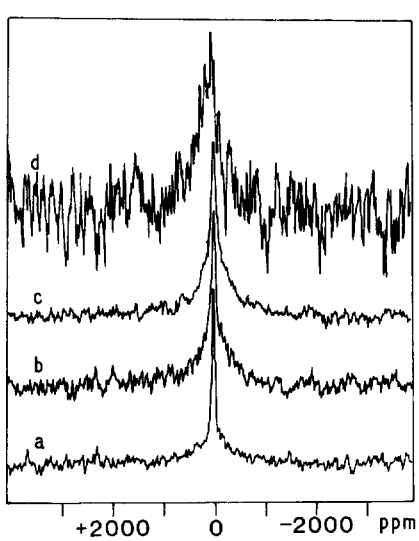

Figure 7. ^{39}K solid state NMR powder spectra of K-montmorillonite paste with 40% w/w clay. Key: a = 0 wetting and drying cycle (W-D) of the original montmorillonite, b = 11 W-D cycles, c = 100 W-D cycles and d = 100 W-D cycles + 4 Sr^{2+} exchanges (Lambert et al. 1982).

is replaced by Sr (Figure 7). More work is needed to identify K that is completely dehydrated and may be no longer exchangeable.

Cadmium-montmorillonite and Cd-hectorite were also studied as a function of water content by Bank and coworkers (Bank, Bank and Ellis 1989; Bank, Bank, Marchetti et al. 1989) and Tinet et al. (1991). The last authors show in particular that Cd in slurries is located in 2 different sites: Cd between clay layers and Cd on external surfaces. The assessment of the amount of Cd in both sites may give indications on the average size of tactoids.

The solid-state NMR study of exchangeable cations may give complementary information on water–cation–clay structure interactions, particularly concerning the distribution of exchangeable cations near clay surfaces. If solid-state NMR spectroscopy is well adapted to study the state and location of exchangeable cations in wet systems, far-IR spectroscopy is more appropriate to study clays at low water contents. Figure 8 gives the far-IR spectra recorded under vacuum of Llano vermiculite saturated by mono- and divalent cations. The 2 peaks observed with Cd probably correspond to 2 different states for that cation: Cd^{2+} and $CdOH^{+}$ (Laperche 1991).

https://doi.org/10.1346/CCMN.1998.0460201 Published online by Cambridge University Press

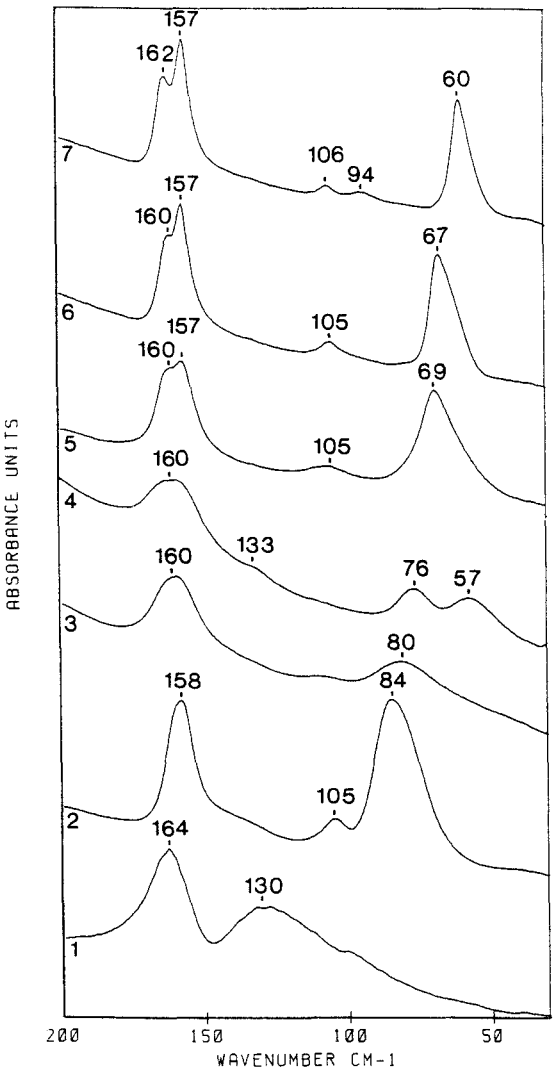

Figure 8. Far-IR spectra of vermiculite saturated by: NH_4^+ (1); K^+ (2); Sr^{2+} (3); Cd^{2+} (4); Ba^{2+} (5); Rb^+ (6); Cs^+ (7) (Laperche 1991).

Water–Cation–Clay Structure Interactions: Structure of Adsorbed Water

The FHH plot of the water desorption isotherm data allows the identification of 2 states of water: water retained by adsorption on hydrophilic sites or on "free surfaces" and water retained by condensation at contact points between particles or in pores (Prost 1990). So 2 mechanisms are involved in the water retention phenomenon: adsorption and capillary condensation. Capillary condensation and multilayer adsorption were already discussed in the preceding pages. Particular attention will be given now to the first steps of the hydration process which are strongly related to the water–cation–clay structure interactions.

Table 2. Interlayer spacing and mean number of water molecules per cation of Cs-, Na- and Ba-hectorite for water content 0.1 g g^{-1}.

	Interlayer spacing *d(001)* (A)	Mean number of water molecules per cation	% RH
Cs-hectorite	12.4	1.6	40
Na-hectorite	12.2	2.3	20
Ba-hectorite	12.5	8.2	15

At the lowest values of a_w water molecules retained by clays are adsorbed on exchangeable cations. The hydrated cations make pillars, inducing an increase of the spacing between clay layers. Table 2 gives the apparent $d(001)$ spacing of Cs-, Na- and Ba-hectorite layers when the water content of the clay is 0.1 g g^{-1} (Prost 1975c) at the corresponding relative humidity. The $d(001)$ spacing is roughly the same for hectorite saturated by Cs, Na and Ba. The mean number of water molecules per cation obtained by dividing the amount of water located in the interlamellar spaces, as determined by IR spectroscopy, by the number of cations (Prost 1990), is a function of its energy of hydration: Cs cations are less hydrated than Na and Ba cations. This result shows that the adsorption of water on clay surfaces does not occur by monolayers as is suggested by the apparent $d(001)$ spacing determined by XRD. The adsorption occurs around each cation, making pillars that fix the interlamellar spacing. If the hypothesis of monolayer adsorption on basal surfaces is accepted, in the case presented here where the accessibility of water to these surfaces is the same for each sample, the coverage of the internal surfaces should be greater with Cs-hectorite than with Ba-hectorite because a_w is much higher in the Cs system. The contrary is observed, showing that the adsorption in this range of the activity of water does not occur on oxygen atoms of basal surfaces but on exchangeable cations (Prost 1990).

In the case of smectites that have their isomorphic substitutions in the octahedral sheet of the layers and where water molecules are not involved in hydrogen bonds with surface oxygen atoms (Prost 1975c), basal surfaces have an hydrophobic character. The hydrophilicity of these clays is only due to the existence in the interlamellar spaces of exchangeable cations. That conclusion is supported by water adsorption isotherms obtained with reduced charge montmorillonite (Calvet and Prost 1971). Indeed the amount of water adsorbed is a function of the charge density of the clay and the nature of the exchangeable cations. This result is in good agreement with the hydrophobic character of talc and pyrophyllite which have no deficit of charge.

In the case of smectites that have their isomorphic substitutions in the tetrahedral sheet of the layer, water molecules adsorbed in the interlamellar spaces are involved in hydrogen bonds with oxygen atoms belong-

https://doi.org/10.1346/CCMN.1998.0460201 Published online by Cambridge University Press

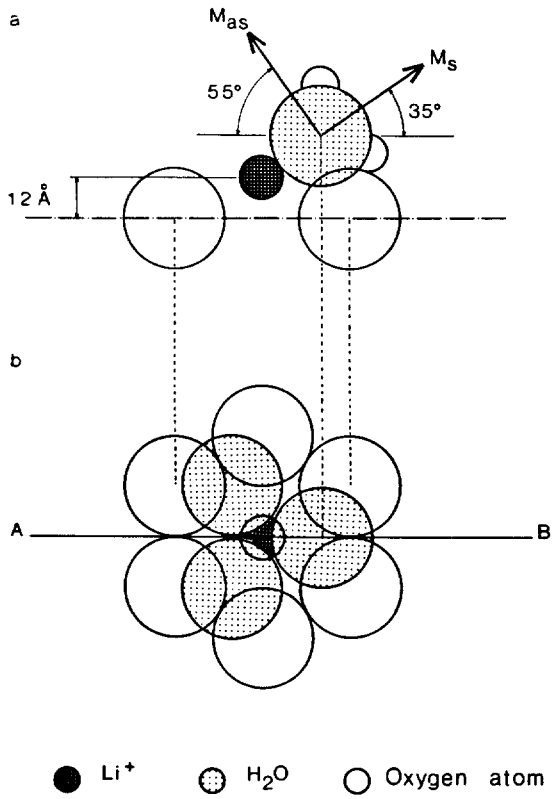

Figure 9. Orientation of the water molecules with respect to Li^+ cation and oxygen atoms of the surface (Prost 1975c).

ing to tetrahedra where Si is replaced by Al or Fe. Exchangeable cations are as close as possible to the isomorphic substitutions and only water molecules that hydrate cations can be involved in such hydrogen bonds. In minerals whose isomorphic substitutions are located in the tetrahedral sheet of the layer, hydrogen bonds between water and oxygen atoms of the structure may explain the generally stronger water–clay structure interactions observed and the limited expansion of the layers.

If domains without any charge exist on the surface there will be no adsorption of water molecules. Indeed, clays saturated by methyl- or trimethyl ammonium cations do not adsorb water.

Structure of Adsorbed Water

Schematic representations of the arrangement of water molecules with respect to basal surfaces and to exchangeable cations are now presented. Figure 9 shows the arrangement of water molecules in the case of Li-hectorite, whose isomorphic substitutions are located in the octahedral sheet of the layer. The exchangeable cations are hydrated by 3 water molecules when the sample is under vacuum (Prost 1975c). Water molecules are not involved in hydrogen bonds with the oxygen atoms of the surface, and their plane is perpendicular to the plane of the structure with 1 proton directed to the center of the hexagonal holes. Figure 10 shows the arrangement in the case of Ca-saponite whose isomorphic substitutions are located in the tetrahedral sheet of the layer. Here water molecules have 1 OH group involved in a hydrogen bond with oxygen atoms of the surface belonging to tetrahedra where Si^{4+} is replaced by Al^{3+} (Suquet et al. 1977).

The question of whether there is a long-range effect of clay basal surfaces and compensating cations on the structure of water still remains an object of controversy. Low (1979), analyzing thermodynamic data, arrived at the conclusion that there is a long-range effect of basal surfaces on the structure of adsorbed water. That conclusion is questionable because thermodynamic data should be related to both phases: clay layers and water (Sposito and Prost 1982). Mulla and Low (1983) analyzed IR spectroscopic data of adsorbed water and concluded again that a long-range effect of basal surfaces on the structure of water exists, based on an exponential change in the extinction coefficient of adsorbed water. The spectroscopic approach has the advantage, compared to the thermodynamic one, of giving information that is specific to adsorbed water; however, the exponential change of the extinction coefficient of adsorbed water can also be explained by the existence of 2 kinds of water molecules whose extinction coefficients are different.

The discontinuous model for adsorbed water, that is to say the existence of 2 kinds of water molecules, one corresponding to water molecules which hydrate exchangeable cations and the other adsorbed on the surface covered by hydrated cations, is supported by an experiment performed in the near-IR range, where the difference of the extinction coefficient of both kinds of water molecule is much less important (Luck 1973). It was found (Prost 1982) that the spectrum of water adsorbed on Na-hectorite can be decomposed into the spectrum of adsorbed water at a water content of 0.5 g g^{-1} and the spectrum of bulk water. This experiment and others performed with different spectroscopies, for example NMR (Fripiat et al. 1982), lead to the conclusion that there are no more than 2 or 3 monolayers of water whose structure is perturbed by the topography of the surface electric field.

THE SWELLING AND SHRINKAGE PHENOMENA

The purpose of this section is to show how the hydration and dehydration processes are related to the swelling and shrinkage phenomena of clay systems.

The Hydration and Dehydration Mechanisms

It was shown in the preceding sections of this paper that the water retention phenomenon has to be related to 2 mechanisms: *adsorption* on hydrophilic sites and on "free surfaces" and *capillary condensation* in

https://doi.org/10.1346/CCMN.1998.0460201 Published online by Cambridge University Press

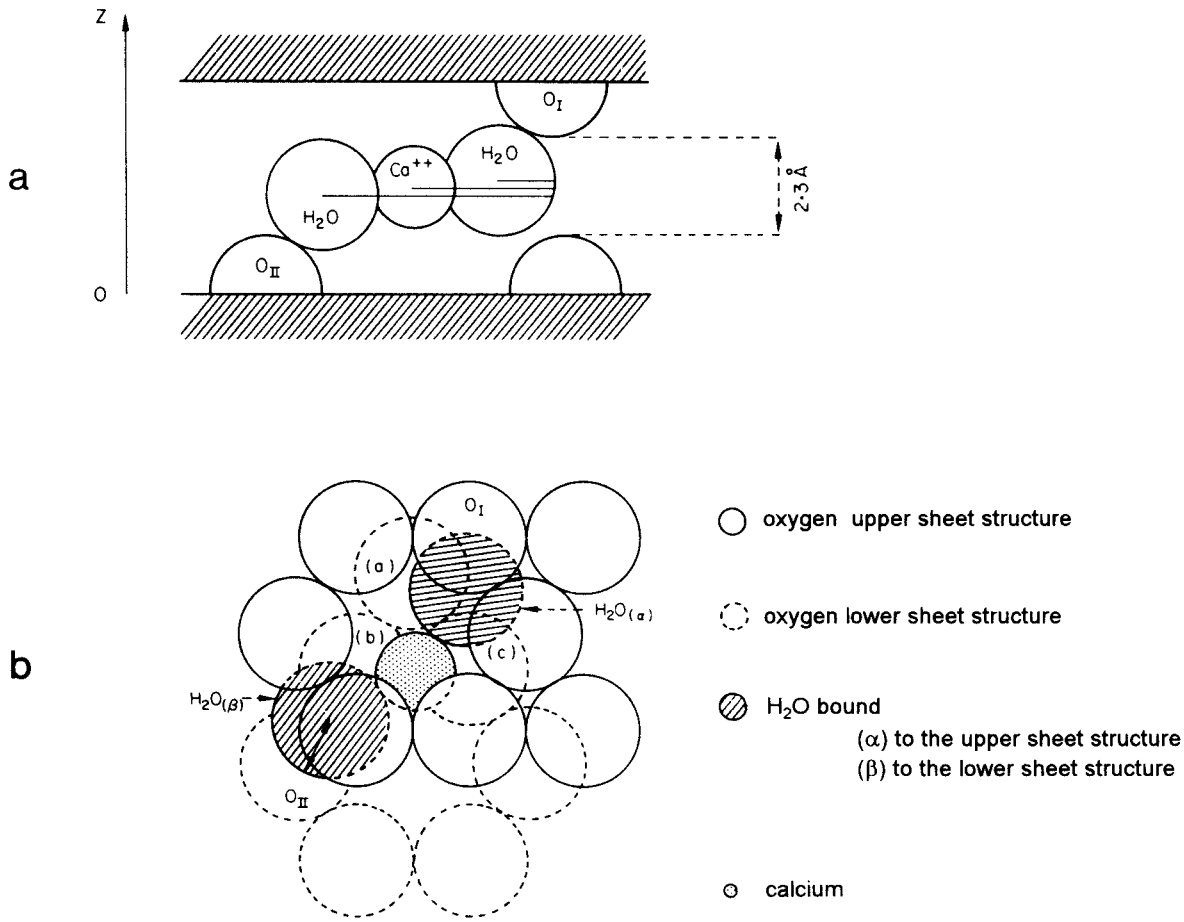

Figure 10. Spatial arrangement of water molecules solvating exchangeable Ca^{2+} on saponite as determined by XRD and IR spectroscopy. a) section view; b) plan view showing water molecules hydrogen-bonded to oxygen atoms in an upper silicate surface (O_I) and to oxygen atoms in a lower silicate surface (O_{II}) bounding the interlamellar space (Suquet et al. 1977).

pores, which are a consequence of the fabric of particles or grains that make the paste. At the lowest values of a_w adsorption occurs on hydrophilic sites (exchangeable cations in smectites, surface OH groups in oxides, . . .). In smectites, hydrated cations make pillars which expand the layers. This is strongly supported by the increase by steps of the $d(001)$ spacings of the layers which is specific, for each value of a_w, to the nature of the exchangeable cation. Except in a few cases, such as Na, the $d(001)$ spacing is limited to around 2 nm in clays that have their isomorphic substitution in the octahedral sheet of the layer and to around 1.5 nm in clays that have their isomorphic substitution in the tetrahedral sheet of the layer, even for the highest water contents. The explanation lies in the nature of specific water–cation–clay structure interactions.

With Ca-clays, pillars are made of the cations hydrated by 6 or more water molecules (Suquet et al. 1977). In the case of clays that have their isomorphic substitution in the tetrahedral sheet of the layers, water molecules are involved in hydrogen bonds with oxygen atoms belonging to tetrahedra where Si is replaced by Al or Fe (Prost 1975a, 1975c; Sposito and Prost 1982). Hydrated Ca ions act as snaps between layers, avoiding a larger expansion. In the case of clays that have their isomorphic substitution in the octahedral sheet of the layer, water molecules that hydrate Ca are not involved in hydrogen bonds and may have a different orientation with respect to the lattice, making the complete hydration of Ca cations easier. As a consequence, pillars are bigger and induce a larger but always limited expansion. With clays that have their isomorphic substitutions in the octahedral sheet of the layers and cations that may have more than 2 shells of hydration, such as Na, pillars are so big that they induce an unlimited expansion. Macroscopic data concerning swelling are reported and analyzed by Low (1979, 1980). Data obtained at the molecular level are needed for a better explanation of the X-ray and heat of immersion results discussed by Low.

https://doi.org/10.1346/CCMN.1998.0460201 Published online by Cambridge University Press

The water molecules that hydrate cations and make pillars between the layers may join together and, depending on the density of charge, may cover the surface completely or partially. Areas of the surface that are not covered by hydrated cations are hydrophobic. As a_w increases to reach domain 2 of the FHH plot, adsorption may be described as a multilayer adsorption process; that is to say, the adsorption of successive layers of water on a film of water made of the hydrated hydrophilic sites. This multilayer adsorption process occurs on "free surfaces" (walls of unsaturated pores or surfaces of stacked layers, particles, aggregates that are free to expand). The multilayer adsorption process occurs until $a_w = 1$. It does not mean necessarily that the structure of water adsorbed according to this process is affected by the surface. This picture is in agreement with the idea that only a limited number (around 4) of layers of water adsorbed on clay surfaces are perturbed by clay surfaces. These first layers of water whose structures are perturbed by the surface correspond to water that hydrates hydrophilic sites.

The water retention phenomenon is due to adsorption and to capillary condensation. This last phenomenon may occur for very low values of a_w at contact points between particles or aggregates, and for higher values of a_w in pores that are the result of the fabric of wet particles or aggregates. If the material is made of homodisperse grains, the constriction radius of the pores will correspond to narrow peaks on the pore size distribution curve and the emptying of pores will occur in a small range of a_w (Figure 4).

Both mechanisms, adsorption and capillary condensation, may occur in the whole range of the activity of water but each state of water, adsorbed or condensed, may be predominant in some particular range of a_w. The FHH plot can be used to assess the amount of water retained by finely divided materials, and belonging to both states. The amount of water retained by adsorption is a function of the surface area where the adsorption mechanism occurs, but the amount of water retained by capillary condensation is a function of the shape of the particles. For example, well-dispersed smectites (Na-montmorillonites) have a very low amount of water retained by capillary condensation. As a consequence, the states and location of water are strongly related to the concepts of surface and fabric of particles or aggregates which make the paste.

The Concept of Surface

Taking the case of Ca-montmorillonite as an example, Figure 11a gives a schematic representation of the different surfaces involved in water retention. The beginning of the hydration process occurs on Ca cations. The amount of water retained here is a function of the surface charge density. The surface involved is the total surface area S_t of the clay which can be assessed by ethylene glycol adsorption experiments or by calculation.

The cation–water–clay structure interactions in the overlapping area of adjacent particles of Ca-montmorillonite are the same as for interlamellar spaces. Hydrated Ca cations located between these overlapping areas act, as they do in the interlamellar spaces, as snaps that limit expansion. As a consequence, hydrated Ca-aggregates have a rigid porous structure. The limited expansion of the layers as a_w increases implies that the multilayer adsorption of water occurs for higher values of a_w on "free surfaces". The surface area S_s, which has to be considered at these low values of a_w, can then be determined by the application of the BET formalism to the nitrogen adsorption isotherm.

As the capillary condensation phenomenon has filled these intraaggregate pores, adsorption can only occur on "free surfaces" which are the external surfaces of aggregates. This surface area S_e is determined by hydraulic conductivity measurements (Prost 1990).

Thus 3 kinds of surface—S_t, S_s and S_e—are involved to explain the adsorption of water. The area of each kind of surface is determined by a specific technique.

The Concept of Fabric

The fabric is the way particles and aggregates are arranged in the paste. The hydraulic conductivity measurements performed on saturated materials (domain 4 of the FHH plot) give the mean hydraulic radius of the pores, that is to say, half the mean distance between "free" particles or aggregates (Figure 11b). The application of the Pierce formalism (Pierce 1953) to the domain of the water desorption isotherm that corresponds to desaturation of the paste (domain 3 of the FHH plot) gives the pore size distribution curve of wet materials. The application of such a formalism implies the knowledge of the thickness t of the film of water adsorbed on "free surfaces" as a function of a_w. The very good consistency of the results obtained with Al_2O_3 grains using both techniques is observed in Figure 12. It indicates that the mean distance between particles decreases linearly as a function of water content. Our hypothesis is that the distance between grains at contact points is equal to twice the thickness t of the film of water adsorbed on external surfaces of particles or aggregates (Figure 11b). Thus the thickness t of the film of water adsorbed on external surfaces of particles or aggregates fixes the distance between particles and aggregates as a function of a_w.

The t-Curve

The t-curve is the plot of the thickness t of the film of water adsorbed as a function of a_w. Hagymassy et al. (1969) have determined the t-curve for different finely divided oxides using water adsorption isotherms obtained by the desiccator method ($a_w < 0.98$). Data plotted on Figure 13 correspond to domain 2 of the

https://doi.org/10.1346/CCMN.1998.0460201 Published online by Cambridge University Press

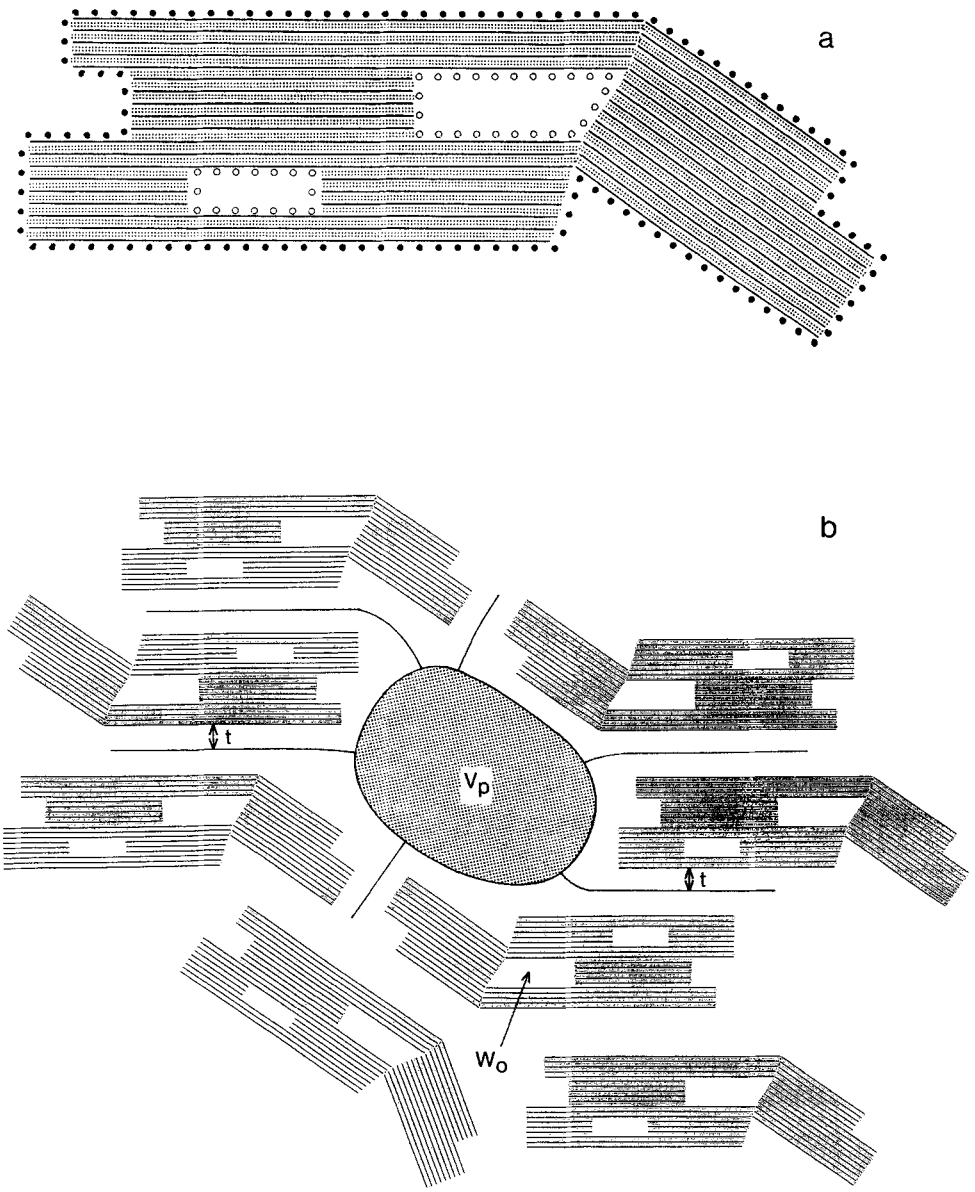

Figure 11. Schematic representation of the fabric of Ca-smectite pastes. a) Individual aggregate of Ca-smectite showing the different surfaces involved in the water retention phenomenon: the total surface area S_t corresponds to surfaces labeled by ●●●, ○○○, and ▪▪▪; the specific surface area S_s, determined by nitrogen adsorption, corresponds to surfaces labeled by ●●● and ○○○; the external surface area S_e of aggregates, determined by hydraulic conductivity, corresponds to surfaces labeled by ●●●. b) Arrangement of individual aggregates showing how swelling is induced by the increase of the thickness t of the layer of water adsorbed on the external surfaces S_e of aggregates; w_o corresponds to water located in the interlamellar spaces and in the intraaggregate pores. V_p corresponds to water located in interaggregate pores.

FHH plot where the multilayer adsorption process is predominant (Benchara 1991). The mean curve calculated from these data leads to the following equation:

$$t(\text{nm}) = \frac{0.24}{(\log(1/a_w))^{0.36}} \quad [3]$$

The t values calculated for the highest values of a_w with this equation are in good agreement with experimental data obtained by Derjaguin et al. (1987) using ellipsometry for $0.97 < a_w < 1$. It is noticeable that t-curves obtained are quite close to each other for materials whose density of surface hydrophilic sites is sufficient to cover the surface with a layer of water when these sites are hydrated. It seems that the effect of the substrate on the multilayer adsorption process

https://doi.org/10.1346/CCMN.1998.0460201 Published online by Cambridge University Press

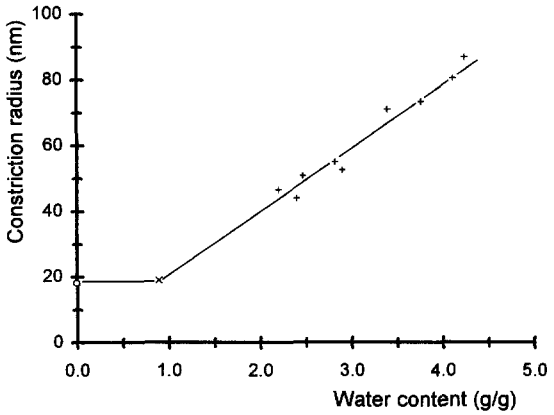

Figure 12. Constriction radii of pores of Al_2O_3 samples as a function of water content. Points (+) were obtained by hydraulic conductivity measurements; (×) by the application of the Pierce formalism to the water desorption isotherm; (○) by mercury injection and by the application of the Pierce formalism to the nitrogen desorption isotherm.

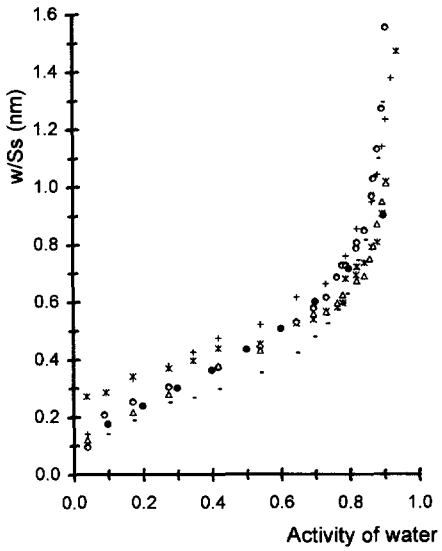

Figure 13. The *t*-curves obtained with different materials: (△) kaolinite; (+) chrysotile; (*) TiO_2; (◇) Al_2O_3; (○) silica A200; (−); silica 280; (●) mean values of *t* taken from Hagymassy et al. (1969). The symbol *w* is the water content and S_s the specific surface area.

is insignificant beyond this first shell of hydration of particles which corresponds to water molecules that hydrate hydrophilic sites.

The Swelling and Shrinkage Mechanisms

Water is retained by finely divided materials according to 2 mechanisms: adsorption and capillary condensation. Water adsorbed at the lowest values of a_w (domain 1) on hydrophilic sites induces the creation of pillars between clay layers that expand the layers and, eventually, results in the creation of a film of water on surfaces. Swelling should be, in that case, related to the total surface area of the clay.

For higher values of a_w the multilayer adsorption process occurs on the film of water that corresponds to the hydration of hydrophilic sites. The thickness *t* of the film of water adsorbed can only increase as a function of a_w if the multilayer adsorption phenomenon occurs on what Pierce (1960) called "free surfaces" (walls of unsaturated pores or surfaces that may move with respect to each other).

Thus, in the case of Ca-montmorillonite, the multilayer adsorption process can occur, at the beginning of domain 2, only on surfaces that are accessible to nitrogen (Figure 11). Because the expansion of Ca-smectite layers with water is limited to around 1 nm, the surface involved in the swelling of such a clay is the external surface area S_e of particles or aggregates, which can be determined by hydraulic conductivity measurements (Prost 1990). So swelling is due to the multilayer adsorption process that occurs on the external surfaces S_e of particles or aggregates and increases the thickness *t* of the film of adsorbed water. This mechanism exists even at the highest values of a_w.

During the multilayer adsorption process, capillary condensation can occur at the lowest values of a_w at contact points of particles or aggregates and at higher values of a_w in pores whose radii satisfy the Kelvin equation. Capillary condensation develops forces that bring particles or aggregates together (Parker 1986). Capillary condensation forces are opposite to adsorption forces. The equilibrium is reached for 1 value of a_w when these forces are equal.

The proposed mechanism to explain swelling or shrinkage was checked in the case of Na-montmorillonites. It was assumed in the case of very well-dispersed Na-montmorillonites that the greatest part of water fixed by the clay is adsorbed. Indeed it is not possible in these clays to identify domain 3 on the FHH plot (Figure 3c). The contribution of capillary condensation to water retention is weak, but strong enough to create opposite forces to adsorption forces. The multilayer adsorption process in well-dispersed Na-montmorillonite occurs on the total surface area of the clay. The amount of water that can be fixed as a function of a_w is calculated by multiplying the total surface area S_t by *t*. It is notable (Figure 14) that the agreement with the experimental data is quite good. It is not so in the case of Ca-montmorillonite, where the external surface area S_e of particles or aggregates is smaller and has to be taken into account for the high values of a_w.

CONCLUSION

The retention of water by clays and finely divided materials is due to adsorption and capillary conden-

https://doi.org/10.1346/CCMN.1998.0460201 Published online by Cambridge University Press

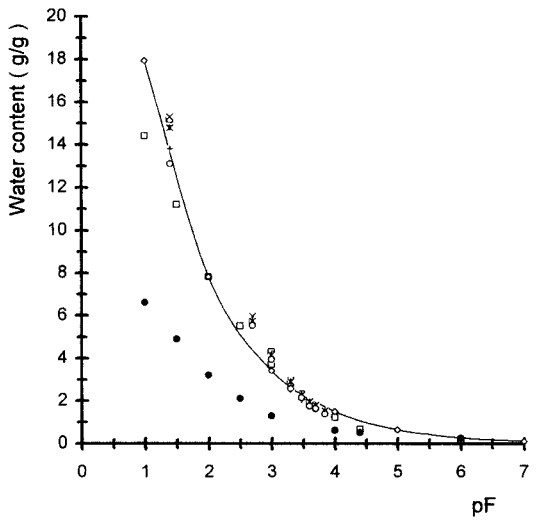

Figure 14. Calculated (–◇–) and experimental (Low 1982; Tessier 1984) water contents as a function of pF in the cases of several Na-montmorillonites (□, +, ×, *, ○) and 1 Ca-montmorillonite (●).

sation. The adsorption creates pillars between clay layers and a water film on external surfaces of particles or aggregates which induce the increase of the spacing between clay layers and of the distance between particles or aggregates. This is the swelling mechanism. Adsorption forces that induce swelling are equilibrated by capillary condensation forces.

The *t*-curves obtained for water seem to be valid for "hydrophilic" materials and can be used to assess their swelling if the external surfaces S_e of particles or aggregates can be determined. The proposed hypothesis to explain swelling and shrinkage is directly related to the concept of external surface S_e of particles or aggregates. This concept underscores the importance of all parameters that are involved in the size of these particles or aggregates. The more important of these parameters is probably, in the case of clays, the cation–water–clay structure interactions and, in particular, the way cations and water molecules are arranged between layers, that is to say the structure of adsorbed water. The ionic composition of the solution may also have a tremendous effect through the dispersion or flocculation process it induces.

ACKNOWLEDGMENTS

We thank J. Driard for finalizing the manuscript and the reviewers for their helpful suggestions.

REFERENCES

Adkins BD, Reucroft PJ, Davis BH. 1986. The FHH multilayer expression: Effects of particle size. Adsorption Sci Technol 3:123–140.

Bank S, Bank JE, Ellis PD. 1989. Solid-state ^{113}Cd nuclear magnetic resonance study of exchanged montmorillonites. J Phys Chem 93:4847–4855.

Bank S, Bank JF, Marchetti P, Ellis PD. 1989. Solid-state cadmium-113 nuclear magnetic resonance study of cadmium speciation in environmentally contaminated sediments. J Environ Qual 18:25–30.

Benchara A. 1991. Etats et localisation de l'eau retenue par des matériaux finement divisés: Mécanismes de l'hydratation et du gonflement [Ph.D. thesis]. Paris, France: Univ Paris 7. 106 p.

Bourrie G, Pedro G. 1979. La notion de pF, sa signification physico-chimique et ses implications pédogénétiques. 1—Signification physicochimique—relation entre le pF et l'activité de l'eau. Sci Sol 4:313–322.

Calvet R, Prost R. 1971. Cation migration into empty octahedral sites and surface properties of clays. Clays Clay Miner 19:175–186.

Carrott PJM, McLeod AI, Sing KSW. 1982. Application of the Frenkel–Halsey–Hill equation to multilayer isotherms of nitrogen on oxides at 77 K. In: Rouquerol J, Sing KSW, eds. Proc Int Symp on Adsorption at the Gas-Solid and Liquid-Solid Interface; 1981; Aix-en-Provence, France. Amsterdam: Elsevier. p 403–410.

Derjaguin BV, Churaev NV, Muller VM. 1987. Surface forces. New York: Plenum Publ. 440 p.

Eisenberg D, Kauzmann W. 1969. The structure and properties of water. Oxford, UK: Clarendon Pr. 296 p.

Frenkel J. 1946. Kinetic theory of liquids. London, UK: Oxford Univ Pr.

Fripiat JJ, Cases JM, Francois M, Letellier M. 1982. Thermodynamic and microdynamic behavior of water in clay suspensions and gels. J Colloid Interface Sci 89:378–400.

Hagymassy J, Brunauer S, Mikhail RSH. 1969. Pore structure analysis by water vapor adsorption. I. *t*-curves for water vapor. J Colloid Interface Sci 29(3):485–491.

Haines WB. 1923. The volume changes associated with variation of water content in soil. J Agric Sci 13:296–310.

Halsey G. 1948. Physical adsorption on non-uniform surfaces. J Chem Phys 16(10):931–937.

Hill TL. 1952. Theory of physical adsorption. Adv Catalysis 4:212–258.

Jurinak JJ. 1963. Multilayer adsorption of water by kaolinite. Soil Sci Soc Proc 27:269–272.

Koutit T. 1989. Mécanismes de l'hydratation des argiles. Etude de l'état et de la localisation de l'eau adsorbée. [Ph.D. thesis]. Rabat, Maroc: Univ of Rabat. 107 p.

Lambert JF, Prost R, Smith ME. 1992. ^{39}K solid-state NMR studies of potassium tecto- and phyllosilicates: the *in situ* detection of hydratable K^+ in smectites. Clays Clay Miner 40(3):253–261.

Laperche V. 1991. Etude de l'état et de la localisation des cations compensateurs dans les phyllosilicates par des méthodes spectrométriques. [Ph.D. thesis]. Paris, France: Univ Paris VII. 100 p.

Laperche V, Lambert JF, Prost R, Fripiat JJ. 1990. High-resolution solid-state NMR of exchangeable cations in the interlayer surface of a swelling mica: ^{23}Na-, ^{111}Cd- and ^{133}Cs-vermiculites. J Phys Chem 94(25):8821–8831.

Low PF. 1979. Nature and properties of water in montmorillonite–water systems. Soil Sci Soc Am J 43:651–658.

Low PF. 1980. The swelling of clay: II. Montmorillonites. Soil Sci Soc Am J 44:667–676.

Luck WAP. 1973. Infrared studies of hydrogen bonding in pure liquids and solutions. In: Franks F, ed. Water: A comprehensive treatise. Water in crystalline hydrates. Aqueous solution of simple nonelectrolytes, Vol 2. New York: Plenum Pr. p 235–321.

Mulla DJ, Low PF. 1983. The molar absorptivity of interparticle water in clay–water systems. J Colloid Interface Sci 95(1):51–60.

https://doi.org/10.1346/CCMN.1998.0460201 Published online by Cambridge University Press

Norrish K. 1954. The swelling of montmorillonite. Disc Faraday Soc 18:120–134.
Parker JC. 1986. Hydrostatics of water in porous media. In: Sparks DL, ed. Soil physical chemistry. Boca Raton, FL: CRC Pr. p 209–296.
Pierce C. 1953. Computation of pore size from physical adsorption data. J Phys Chem 57:149–152.
Pierce C. 1960. The Frenkel–Halsey–Hill adsorption isotherm and capillary condensation. J Phys Chem 64:1184–1187.
Prost R. 1975a. Etude de l'hydratation des argiles: Interactions eau–minéral et mécanisme de la rétention de l'eau. I: Etude d'une zéolite (natrolite) et de deux minéraux fibreux (attapulgite et sépiolite). Ann Agron 26(4):400–462.
Prost R. 1975b. Etude de l'hydratation des argiles: Interactions eau–minéral et mécanisme de la rétention de l'eau. II: Etude d'une smectite (hectorite). Ann Agron 26(5):463–535.
Prost R. 1975c. Interactions between adsorbed water molecules and the structure of clay minerals: Hydration mechanism of smectites. In: Bailey SW, ed. Proc Int Clay Conf; 1975; Mexico City, Mexico. Wilmette, IL: Applied Publ. p 351–359.
Prost R. 1982. Near infrared properties of water in Na-hectorite pastes. In: Van Olphen A, Veniale F, eds. Proc Int Clay Conf; 1981; Bologna and Pavia, Italy. New York: Elsevier. p 187–195.
Prost R. 1990. Relations eau–argile: Structure et gonflement des matériaux argileux. In: Decarreau A, ed. Matériaux argileux. Structure, propriéte et application. Paris, France: Société Française de Minéralogie et de Cristallographie. p 345–386.
Sposito G. 1972. Thermodynamics of swelling clay–water systems. Soil Sci 114:243–249.
Sposito G. 1981. The thermodynamics of soil solutions. Oxford: Clarendon Pr. p 187–208.
Sposito G, Prost R. 1982. Structure of water adsorbed on smectites. Chemical Reviews 82(6):553–573.
Suquet H, Prost R, Pezerat H. 1977. Etude par spectroscopie infrarouge de l'eau adsorbée par la saponite-calcium. Clay Miner 12:113–126.
Tessier D. 1984. Etude expérimentale de l'organisation des matériaux argileux. Hydratation, gonflement et structuration au cours de la dessiccation et de la réhumectation. [Ph.D. thesis]. Paris, France: Univ of Paris VII. Versailles, France: INRA Versailles Pub. 361 p.
Tinet D, Faugere AM, Prost R. 1991. ^{113}Cd NMR chemical shift tensor analysis of cadmium-exchanged clays and clay gels. J Phys Chem 95(22):8804–8807.
Weiss CA Jr, Kirkpatrick RJ, Altaner SP. 1990a. Variations in interlayer cation sites of clay minerals as studied by ^{133}Cs MAS nuclear magnetic resonance spectroscopy. Am Mineral 75:970–982.
Weiss CA, Jr, Kirkpatrick RJ, Altaner SP. 1990b. The structural environments of cations adsorbed onto clays: ^{133}Cs variable-temperature MAS NMR spectroscopic study of hectorite. Geochim Cosmochim Acta 54:1655–1669.

(Received 24 January 1997; accepted 31 March 1997; Ms. 97-010)

https://doi.org/10.1346/CCMN.1998.0460201 Published online by Cambridge University Press